INSTRUMENTATION

Image Artifacts at High Photon Fluence Rates in Single-Crystal NaI(Tl) Scintillation Cameras

Sven-Erik Strand and Ingemar Larsson

Lasarettet, S-221 85 Lund, Sweden

A method that simulates a clinically relevant situation is used to measure the amount of pulse pileup in the gamma image by distinguishing between correctly and incorrectly positioned events. Comparison was then made between responses from different cameras. These investigations show the influence of pileup rejection on counting rate. Pileup effects can be determined for some cameras at such low count rates as about 10,000/sec with a 30% energy window. Parameters affecting the total count rate of the scintillation camera—such as scattering media, source geometry, collimator, and energy window—have been investigated. It is shown that the energy distribution of the photon fluence striking the crystal determines the counting losses and image distortion, rather than the counting rate in the energy window.

The approach described here might fulfill the requirements for a new method to compare scintillation cameras. It is important to note that measurements without scattering medium yield results irrelevant for clinical situations.

J Nucl Med 19: 407–413, 1978

Soon after the introduction of the Anger camera with a single NaI(Tl) crystal, the problem of counting losses became evident. Initial attempts to correct for these losses considered the scintillation camera as a conventional counter (*1–11*).

In interpreting the results from deadtime measurements, it must be realized that the scintillation camera is exposed to an entire energy spectrum of photons. Only a small fraction of the spectrum yields the counting rate in the energy window, and thus contributes to the image. The important relationship between the energy distribution of the photons, activity, and position signals has recently been reported (*12–15*).

This paper deals with basic factors affecting the counting-rate curves recorded with the scintillation camera. A method is proposed to investigate the counting-rate properties of scintillation cameras in a clinically relevant situation.

The probability that two photon absorptions will occur within the resolving time of the scintillation camera increases with the photon fluence rate. The finite limitation is the decay time of the scintillation in the NaI(Tl) crystal. This is approximately 0.23 μsec for 60% of the scintillations and 1.5 μsec for the remaining light (*16*). At high photon fluence rates a considerable fraction of the photons will interact in the crystal before the scintillation of the preceding event has decayed. Pulses with too high an amplitude—the so-called pileup pulses—will thus be generated. If a pileup is caused by two or more Compton events, or by primary photons of low energy, it can generate a pulse that is accepted in the energy window, and a false event is recorded in the image, located somewhere between the original

Received June 28, 1977; revision accepted Oct. 18, 1977.

For reprints contact: Sven-Erik Strand, Radiation Physics Dept., Lasarettet, S-221 85 Lund, Sweden.

TABLE 1. EXPERIMENTAL CONFIGURATIONS

Experiment	Scintillation camera	Collimator (parallel holes)	Energy window (%)	Geometry: Air	Geometry: Water	No. of sources: one	No. of sources: four
A	Searle Pho/Gamma III HP	15,000 holes, LEHR†	35	X		X	
B	Searle Pho/Gamma III HP	15,000 holes, LEHR†	35		X	X	
C	Searle Pho/Gamma III HP	15,000 holes, LEHR†	30		X		X
D	Searle Pho/Gamma III HP	4,000 holes, LEFH‡	30		X		X
E	Searle Pho/Gamma IV	15,000 holes, LEHR†	30		X		X
F	Searle LFOV	39,200 holes, LEAP§	30		X		X
G	Searle LFOV	39,200 holes, LEAP§	30	X*			X
H	General Electric Radicamera 60	20,000 holes, HRLE¶	30		X	X	
I	General Electric Radicamera 60	20,000 holes, HRLE¶	30		X		X
J	General Electric Portacamera	6,300 holes, LEHR†	20		X		X
K	General Electric Maxicamera I	16,000 holes, LEHR†	30		X		X
L	General Electric Maxicamera I	16,000 holes, LEHR†	30	X*			X

* With backscatter from the water in the water tank.
† LEHR: Low energy, high resolution.
‡ LEFH: Low energy, fine holes.
§ LEAP: Low energy, all-purpose.
¶ HRLE: High resolution, low energy.

events. Such false information can be reduced with pileup rejection circuitry. This reduction can be shown with the present method.

MATERIALS AND METHODS

The experimental conditions for the different scintillation cameras, equipped with parallel-hole collimators, are given in Table 1.

The pulse-height distributions of the energy signals were registered with a multichannel analyser (*17,18*).

The crystal was exposed to varying photon fluence rates by placing a high-activity Tc-99m source in front of the scintillation camera. Measurements were performed regularly during the decay. The amount of activity at the start of the measurement was of the order of 400–700 mCi and the performance was studied until the activity had decayed to approximately 0.2 mCi. The radioactive solution was usually in four 10-ml glass bottles placed at the corners of a square with 15-cm sides, as seen in Fig. 1—or, as in some experiments, in one bottle centered in the camera's field of view.

To simulate the scattering conditions of a clinical investigation the source was placed at a depth of 10 cm in a water tank. The tank was cubical, 50 cm per side, with walls of plexiglass. The collimator-to-surface distance was 5 cm.

With analog discriminators connected to the x and y signals, a cross-shaped region of interest was selected in the image between the four sources, as in Fig. 1. The counting rate in this area was measured by an auxiliary scaler. In this way only the performance of the scintillation camera was investigated without any influence from complex digital equipment. The "cross" was placed 15 mm from the edge of each bottle, this distance being approximately equal to the FWHM of the overall resolution of the scintillation camera. At low counting rates the events in the "cross" were mainly due to scattered photons. At higher photon fluence rate misplaced events due to pileup occurred in the "cross." Consequently, the counting rate in the "cross" was called "pileup plus scatter." The counting rate in the total image was designated "total counting rate" giving both correctly and falsely positioned events. The counting

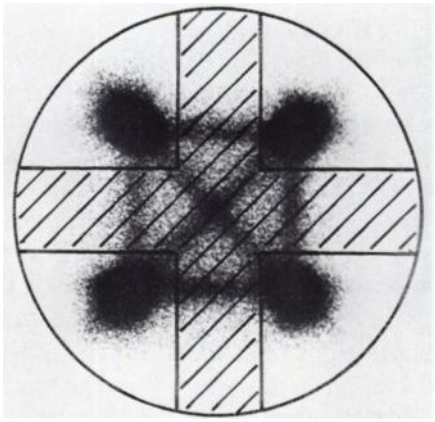

FIG. 1. Region of interest where pileup effect was measured, indicated as a "cross" (shaded region) between the images of the four sources.

rate outside the "cross" was called "with correct position," tolerating a small error because some events due to pileup and scatter are also recorded in this area. At low activities the measured counting rates were fitted to a single exponential curve by the least-squares method. When the exponent agreed with the decay constant of Tc-99m it was assumed that the expression represented the true counting rate.

RESULTS

Pulse-height distribution. From experiments A and B (Table 1) the pulse-height distributions with the source in air and immersed in water are shown in Fig. 2, with activities ranging from 1–170 mCi. At low activity the pulse-height distributions in the two cases differ largely due to attenuation of the primary photons and enhanced Compton scatter in water. The ratio between the counting rate in a given window and the counting rate for the whole pulse-height distribution is indicated in Fig. 3 as a function of window width. The scintillation camera has to process almost the same number of photon events in the two cases (4.4/sec per μCi), although the observed counting rates differ by a factor of 2.

At higher activities the effects of pileup are very prominent in the pulse-height distribution. The high-energy side of the full-energy peak is especially affected. The probability of coincidences of 140-keV photons is much greater with the activity in air than in water, and the sum peak at 280 keV is clearly visible. Above 100 mCi the pulse-height distribution will "collapse" into a continuum.

Studies of pulse-height distributions registered from a scintillation camera at different photon fluence rates obviously give an indication of the count-rate performance of the system. With increasing counting rate, a marked upward shift of the peak depending on the amount of scattering material was observed for one camera (*11*).

Scattering. The influence of scattering on the total counting rate (A and B in Table 1) is shown in Fig. 4A. With the activity in water, the measured counting rates are decreased from the maximum count rate of 74,000/sec to 44,000/sec. The maxima appear at different expected counting rates: 200,000/sec in air compared with 150,000/sec in water. This is because the scintillation camera rejects relatively more pulses when it has to detect the additional scattered photons generated in the water.

In dynamic studies with high activities, the varying number of Compton-scattered photons makes corrections for count losses impossible. Corrections for attenuation will thus be insufficient. For example, detection of an activity of 25 mCi at 100 mm depth would give a counting rate of 27,000/sec with this camera. Allowing for the attenuation, using a correction factor of 3.25 (*19*), 87,750/sec (= 27,000

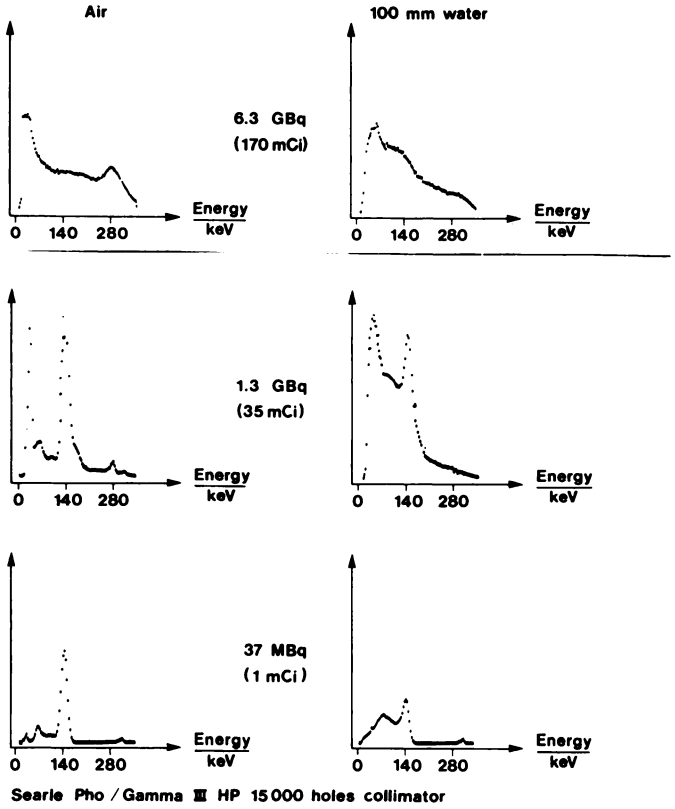

FIG. 2. Pulse-height distributions obtained with source free in air and immersed 100 mm in water. Influence of pileup can be seen at high activities.

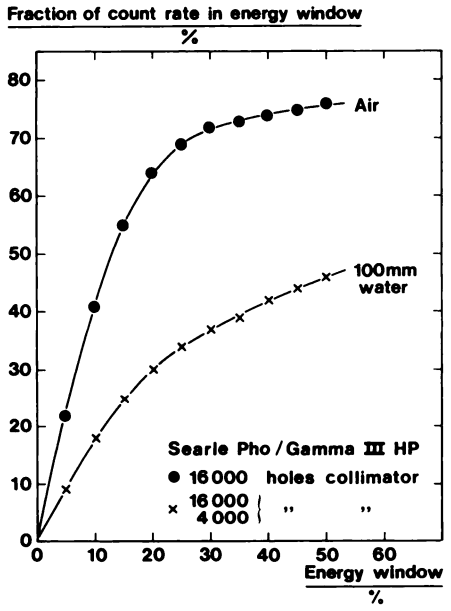

FIG. 3. Pulse rates passing through energy windows of various widths (symmetrically centered over the primary peak), expressed as fractions of the counting rate for the whole pulse-height distribution. Curves obtained with low-activity source free in air and at 100 mm depth in water.

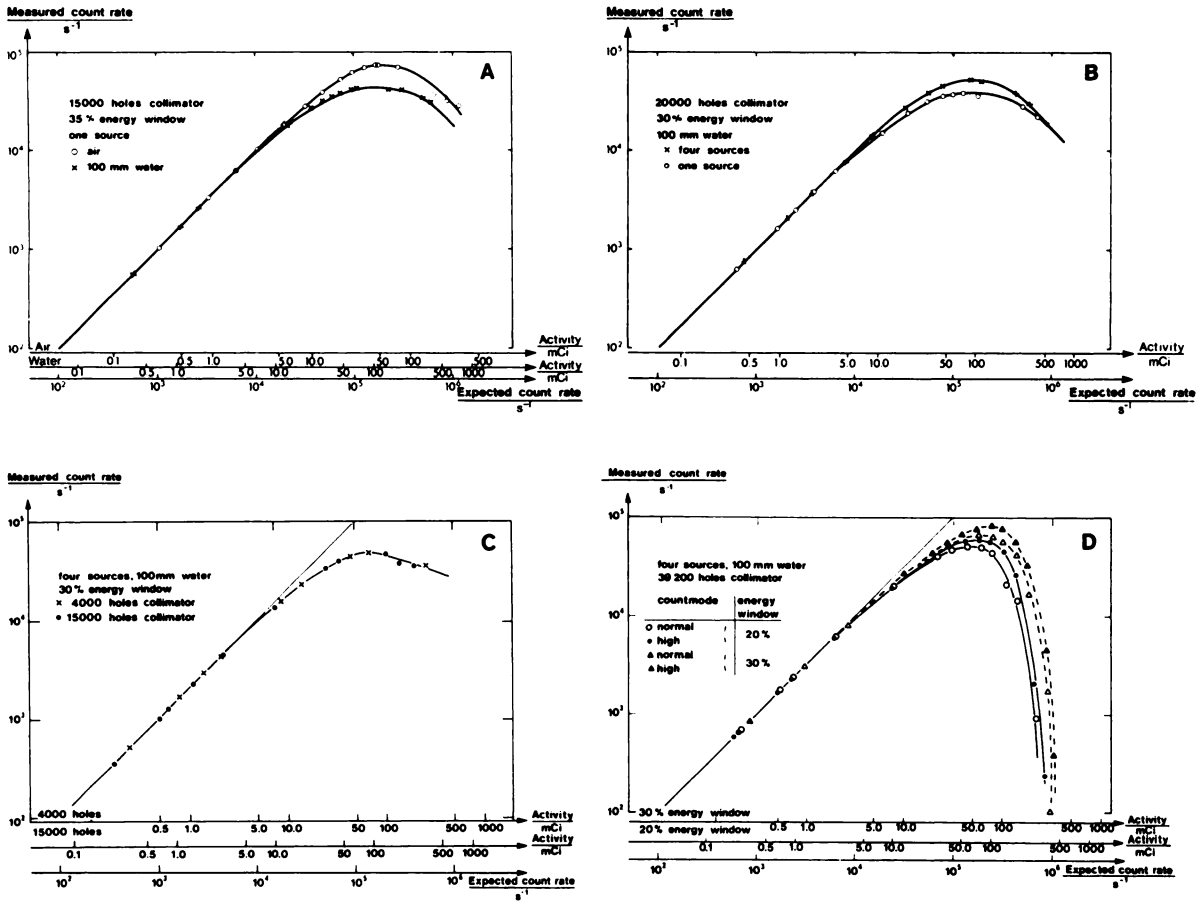

FIG. 4. Measured counting rates from the whole image as a function of expected counting rates. (A) Source free in air and at 100 mm depth in water. (B) Activity concentrated in one source, and divided into four sources. (C) Scintillation camera with two different collimators, with 4,000 and with 15,000 parallel holes. (D) Curves for 20% and 30% energy windows, and for pulse-processing times of 0.5 and 0.9 μsec.

× 3.25) would have been expected. The same activity actually measured in air, however, would give a count rate of 61,000/sec. Thus the "corrected" counting rate is in error by 44%.

Source geometry. The count-rate characteristics for a camera with two different source configurations (H and I in Table 1) are shown in Fig. 4B. A single source yields lower counting rates than four sources with the same total activity, especially at higher activities; maximum counting rate with one source is 39,000/sec compared with 52,000/sec obtained with multiple sources. With the activity concentrated in one source, fewer PM tubes are observing a higher frequency of scintillations, causing greater saturation in these tubes.

Assume that 25 mCi is administered to a patient as a concentrated bolus. At 10 cm depth, this would yield a counting rate of 26,000/sec, or 27% lower than the counting rate of 33,000/sec obtained if the same activity were concentrated in four sources.

Collimation. The energy distribution of the photons that strike the crystal depends on the collimator. This is apparent when the solid angle differs or when septal penetration becomes serious (*18*). Figure 4C shows the count-rate curves for one camera (C and D in Table 1) equipped with two different parallel-hole collimators: (a) with 4,000 square holes, 2 × 2 × 45 mm (equivalent diameter 3 mm); and (b) with 15,000 triangular holes, length 29 mm (equivalent diameter 1.5 mm). No significant differences were observed between the curves because of the small difference in total solid angle for the two collimators and the negligible septal penetration by the 140-keV photons.

Energy window. For one camera (F in Table 1) the count-rate curves were obtained for two different energy windows, 20% and 30%. The processing time in the camera for the energy pulse could be altered by changing the integrating time prior to pulse-height analysis: 900 ns in normal count mode, 500 ns in high-count mode. The results are given in Fig. 4D. With an increase in window opening from 20%

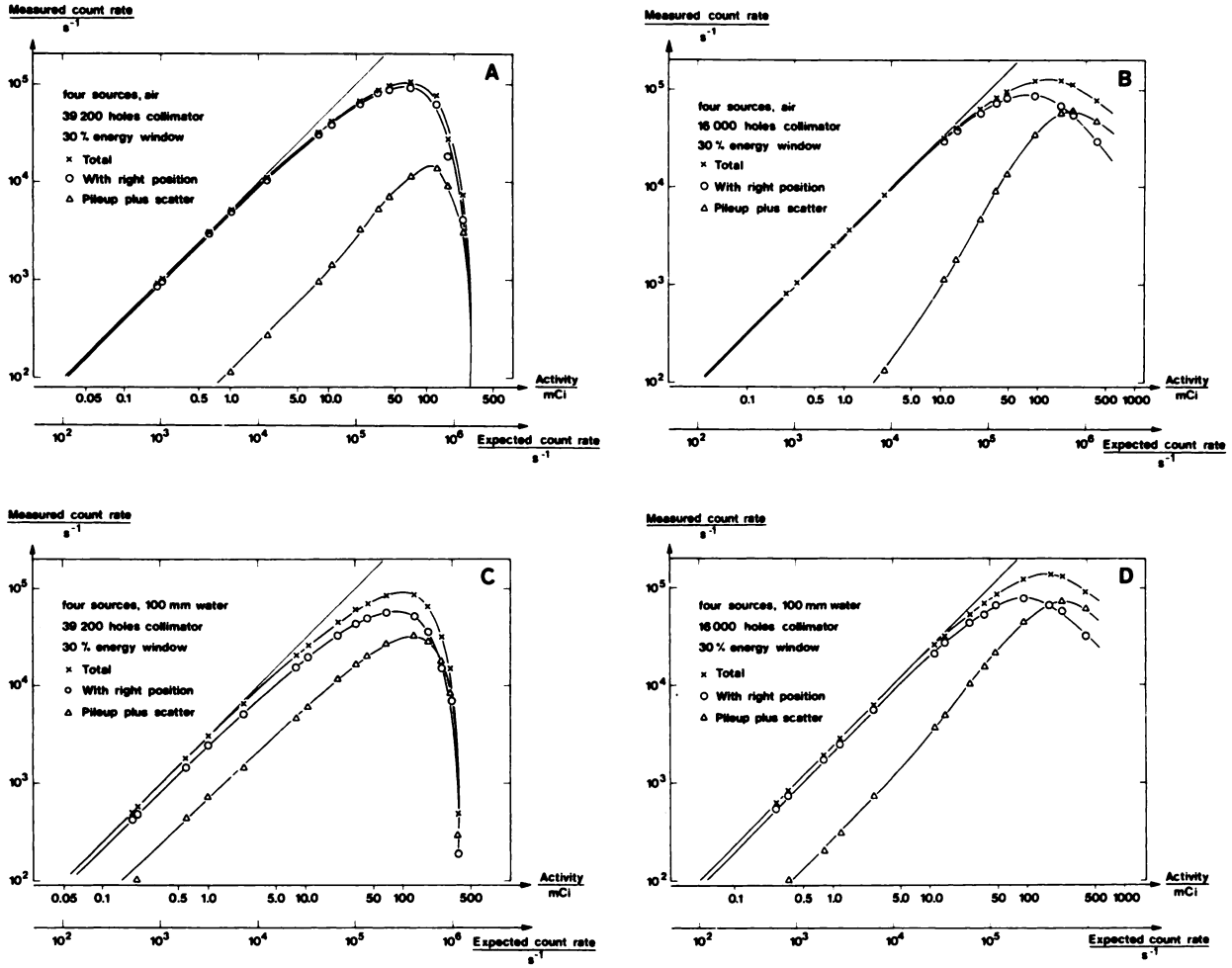

FIG. 5. Count-rate curves for two scintillation cameras with large field of view. The camera in A and C is equipped with pileup rejection circuitry. Curves in A and B had four sources, located above the water; for C and D they were immersed 100 mm deep. Effect of pileup rejection is most clearly seen at high count rates on the curve "pileup plus scatter."

to 30%, the sensitivity is improved by approximately the same amount: 51,000/sec to 67,000/sec for normal-count mode and 61,000/sec to 81,000/sec for high-count mode, respectively. The maxima fall at almost the same activity. A change of pulse-processing time from 900 ns to 500 ns increases the maximum count rate by 20%, and it is obtained at somewhat higher activities.

Pileup. Figure 5 shows the results of the pileup effect in two scintillation cameras with large fields of view (F, G, K and L in Table 1). The curves in Figs. 5A and B were obtained with the activity placed immediately above the water surface. Figure 5A shows count-rate curves that are almost parallel. A small deviation can be observed in the curve "pileup plus scatter," indicating that a minor part is originating from pileup. The major part of the observed counting rates are either correctly positioned or scattered photons. These curves were obtained from a camera with pileup-rejection circuitry. Without pileup rejection (Fig. 5B), a stronger pileup effect is evident because the curve "pileup plus scatter" increases more than the activity would indicate. The curve for correctly placed events reaches its maximum at about 50 mCi. Although a higher maximum total count rate is obtained, compared with Fig. 5A, only 40% of these events are correctly positioned compared with 80%.

Measurements performed with the source at 100 mm depth in the water tank are plotted in Figs. 5C and D. The pileup effect here is partly masked by more numerous Compton-scattered photons, especially in Fig. 5C. In Fig. 5D, however, pileup is evident as soon as the activity exceeds 5 mCi.

Table 2 summarizes some of the findings of the study.

A quantitative measure of the pileup effect can be obtained by dividing the counting rate "with correct

TABLE 2. MEASURED COUNTING RATES

Experiment referred to in Table 1	Counts/sec				Source activity (mCi)
	Maximal "total"	"With correct position"	"Pileup plus scatter"	Expected	
C	47,000	37,000	10,000	130,000	85
E	56,000	41,000	15,000	145,000	120
J	140,000	46,000	94,000	460,000	390
G	105,000	95,000	10,000	330,000	65
L	130,000	83,000	47,000	400,000	125
F	90,000	58,000	32,000	300,000	95
K	135,000	72,000	63,000	360,000	150

position" by the "total" counting rate. At low photon fluence rates,

$$r = \frac{\text{"Total"-"Scatter"}}{\text{"Total"}}$$

is equivalent with the fraction of the total counting rate measured outside the "cross" and l-r is the fraction of the photons scattered and recorded in the "cross." The ratio r is dependent on the centering of the energy window over the full energy peak and on the discriminator setting defining the distance between the edge of the bottle and the "cross." Measurement shows that moving this discriminator ±5 mm alters the ratio by ±3%. The ratio lies in the range 0.8–0.9 with the source in water and, because of reduction of scattering, rises to about 0.98 when the activity is placed immediately above the water surface. This ratio r is normalized to unity at low counting rates to eliminate this difference in scattering into the cross in the different experiments. Thus the normalized ratio is obtained according to

$$R = \frac{\text{"With correct position"}}{\text{"Total"}} \cdot \frac{1}{r}.$$

The figures obtained at higher counting rates therefore reflect the amount of pileup measured in the "cross." These results are plotted as a function of the expected counting rates in Fig. 6. The improvement with pileup rejection is clearly evident. The increase in pileup with scattering is also observed. In Fig. 6, pileup effect can be seen already at 10,000/sec.

At an expected count rate of 70,000/sec, about 5–15% of the "total" counts are pileup events. This corresponds in some of the experiments to an activity level of 30 mCi.

CONCLUSION

High photon fluence rates will give pileup effects in clinical studies. Corrections for image distortion and count losses are thus almost impossible to perform. Pileup rejection reduces the image distortion. The pileup effect varies with the amount of photon scattering, and during a dynamic study it can vary

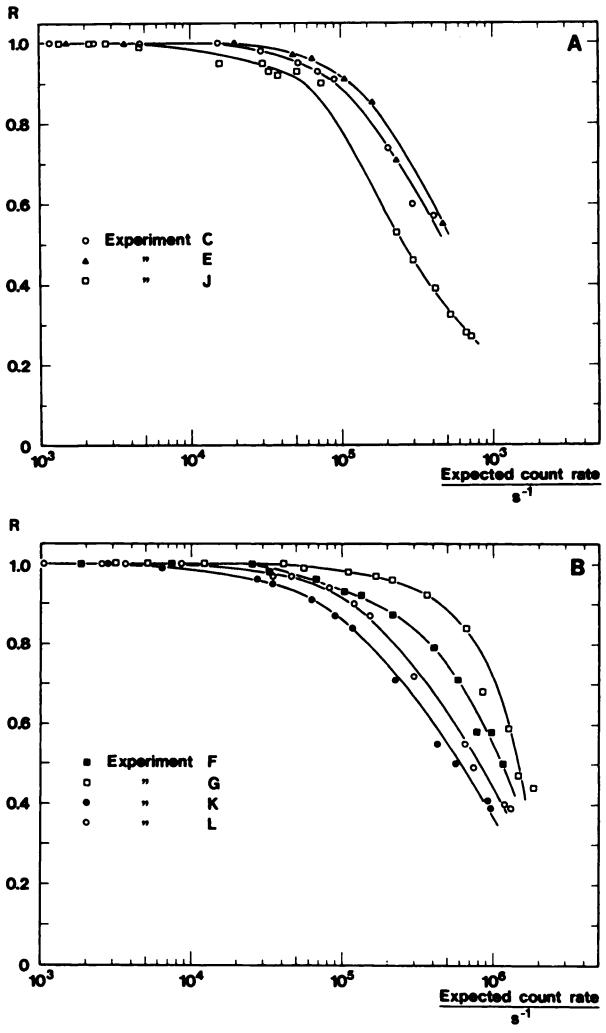

FIG. 6. R = correctly placed counts, as a fraction of total counts, the latter normalized to unity at low source activity. (A) Cameras with field of view 25 cm in diameter; (B) those with 40 cm field. See Table 1 for details. Curves F and G refer to camera with pileup rejection.

with the geometrical distribution of the source.

The temptation to use large activities with very-short-lived radionuclides can cause very troublesome pileup effects. The crucial feature in dynamic studies is not a high image quality but a good statistical confidence level for quantitative data. By use of a wider energy window, adequate counting rates can be achieved while still retaining acceptable image quality (*11*).

The camera's circuitry should be faster than the decay time of the scintillation, thus making only the physical properties of the crystal itself the limiting factor for the counting rate.

The larger the fraction of the whole pulse-height distribution rejected by a single-channel analyzer, the lower the maximal registered counting rate will be. It may be possible to reduce the recording of undesirable photons, however, by means of specially made attenuating filters (*9*) or by combining various detector materials (*20*).

The simple parameter "deadtime" has no practical application in a complicated procedure like scintillation-camera imaging. Maximum total obtainable count rate in the whole image, sometimes used to characterize the count-rate performance of scintillation cameras, is of little value, since it does not distinguish between correctly and wrongly positioned events.

The procedure described here makes this distinction. The most informative presentation of the count-rate performance of a scintillation camera is a family of count-rate curves, as in Fig. 5. The ratio R in Fig. 6—i.e., the fraction of wrongly positioned events—provides complementary information.

ACKNOWLEDGMENTS

Thanks are due to B. Blad and K. Jönsson for valuable help and fruitful discussions on electronics. Also the technical help by Kaj Lange is acknowledged.

This study was supported by grants from the John and Augusta Persson Foundation for Medical and Scientific Research, Lund, Sweden.

A brief summary of this investigation was presented at the poster session of 15th International Annual Meeting of the Society Nuclear Medicine, Groningen, Sept. 13–16, 1977.

REFERENCES

1. ADAMS R, ZIMMERMAN D: Methods for calculating the deadtime of Anger camera systems. *J Nucl Med* 14: 496–498, 1973

2. ADAMS R, JANSEN C, GRAMES GM, et al: Deadtime of scintillation camera systems—Definitions, measurements and applications. *Med Phys* 1: 198–203, 1974

3. PAYNE JT, WILLIAMS LE, PONTO RA, et al: Comparison and performance of Anger cameras. *Radiology* 109: 381–396, 1973

4. ARNOLD JE, JOHNSTON AS, PINSKY SM: The influence of true counting rate and the photopeak fraction of detected events on Anger camera deadtime. *J Nucl Med* 15: 412–416, 1974

5. SORENSON JA: Deadtime characteristics of Anger cameras. *J Nucl Med* 16: 284–288, 1975

6. MORETTI J-L, MENSCH B, GUEY A, et al: Comparative assessment of scintillation camera performance. *Radiology* 119: 157–165, 1976

7. ADAM WE, BITTER F, KAMPMANN H, et al: Grundsätzliche Aspekte der Funktionsscintigraphie. *Proceedings of the International Annual Meeting of the Society of Nuclear Medicine*, 10–13 Sept., 1975, Copenhagen

8. SORENSON JA: Methods of correcting Anger camera deadtime losses. *J Nucl Med* 17: 137–141, 1976

9. MEUHLLEHNER G, JASZCAK RJ, BECK RN: The reduction of coincidence loss in radionuclide imaging cameras through the use of composite filters. *Phys Med Biol* 19: 504–510, 1974

10. IINUMA TA, FUKUHISA K, MATSUMOTO T, et al: Dynamic performance of scintillation camera—computer system and correction for counting—loss due to resolving time. *Proceedings of the First World Congress of Nuclear Medicine*, 1974, Tokyo, pp 151–155

11. MURPHY P, ARSENEAU R, MAXON E, et al: Clinical significance of scintillation camera electronics capable of high processing rates. *J Nucl Med* 18: 175–179, 1977

12. LANGE D, KOBER B, SCHENCK P, et al: Totzeitverluste und pile-up bei hohen Zaehlraten in Scintillationskameras. In *Radioactive Isotope in Klinik und Forschung*, Vienna. Höfer R, ed. Verlag H Egerman, 1976, pp 557–568

13. LANGE D, HERMANN HJ, WETZEL E, et al: Critical parameters to estimate the use of a scintillation camera in high dose dynamic studies. *Proceeding of Fifth Symposium on Medical Radionuclide Imaging*. IAEA, 25–29 Oct., 1976, Los Angeles, pp 85–97

14. STRAND SE, LARSSON I: *Proceeding of Fifth Symposium on Medical Radionuclide Imaging*. Discussion. IAEA, 25–29 Oct., 1976, Los Angeles, pp 98–100

15. STRAND SE, LARSSON I, LAMM IL: Count losses and image distortion at high photon fluence rates (in Swedish). In *Proceeding of Swedish Association of Physicists in Medicine*, Ann. Meeting Stockholm, Sweden, Dec, 1976

16. BIRKS JB: *The Theory and Practice of Scintillation Counting*. Pergamon Press, Oxford, 1964, p 453

17. STRAND S-E, PERSSON BRR: The dual photopeak-area method applied to scintillation camera measurements of effective depth and activity of in vivo ^{123}I distributions. *Europ J Nucl Med* 2: 121–128, 1977

18. BOLMSJÖ M, PERSSON BRR, STRAND SE: Imaging ^{123}I with a scintillation camera. A study of detection performance and quality factor concepts. *Phys Med Biol* 22: 266–277, 1977

19. PERSSON BRR, STRAND SE, WHITE T: 99Tcm-Ascorbate; Preparation, quality-control and quantitative renal uptake in man. *Int J Nucl Med Biol* 2: 113–122, 1975

20. Harshaw Scintillation Phosphors, The Harshaw Chemical Company, 1975, pp 49–50